Design of fractional MOIF and MOPIF controller using PSO algorithm for the stabilization of an inverted pendulum-cart system

Fatima Cheballah, Rabah Mellah, Abdelhakim Saim

Received: 12 October 2023 | Revised: 18 February 2024 | Accepted: 13 March 2024

IET Control Theory & Applications

DOI: 10.1049/cth2.12648

The Institution of Engineering and Technology WILEY

ORIGINAL RESEARCH

Design of fractional MOIF and MOPIF controller using PSO algorithm for the stabilization of an inverted pendulum-cart system

Fatima Cheballah[1] | **Rabah Mellah**[1] | **Abdelhakim Saim**[2]

[1]Laboratoire de Conception et Conduite des Systèmes de Production (L2CSP), University Mouloud Mammeri of Tizi Ouzou, Tizi Ouzou, Algeria

[2]Institut de Recherche en Energie Electrique de Nantes Atlantique, Nantes University, Saint Nazaire, France

Correspondence
Abdelhakim Saim, Institut de Recherche en Energie Electrique de Nantes Atlantique, Nantes University, Saint Nazaire 44600, France.
Email: Abdelhakim.Saim@univ-nantes.fr

Abstract

The topic of this paper is the design of two fractional order schemes, based on a state feedback for linear integer order system. In the first one of the state feedback is associated with a fractional order integral (I^{α}) controller. In the second structure the state feedback is associated with a fractional order proportional integral (PI^{α}) controller. With such controllers, the closed loop system with state feedback described by the state equations splits in n-subsystems with different fractional orders derivatives of the state variable. In order to find the optimal parameters value of both controllers (I^{α}) and (PI^{α}), a multi-objective particle swarm optimization algorithm is used, with the integral of absolute error, the overshoot M_p, the Buslowicz stability criterion are considered as objective functions. The multi-objective integral fractional order controller and the multi-objective proportional integral fractional order controller are applied to stabilize the inverted pendulum-cart system (IP-C), and their performance is compared to the fractional order controller. The simulation results of these innovative controllers are also compared with those obtained by conventional proportional–integral–derivative and fractional order proportional–integral–derivative controllers. The robustness of the proposed controllers against disturbances is investigated through simulation runs, considering the non-linear model of the IP-C system. The obtained results demonstrate that our approach not only leads to high effectiveness but also showcases remarkable robustness, supported by both simulation and experimental results.

1 | INTRODUCTION

1.1 | Literature review

The inverted pendulum-cart (IP-C) system has long been a challenging control problem due to its inherent instability and non-linearity. Traditionally, classical control methods such as proportional–integral–derivative (PID) and linear quadratic regulator (LQR) have been employed [1–3]. However, these methods may fall short in providing satisfactory performance. In recent years, there has been a growing interest in the application of fractional-order control (FOC) techniques for inverted pendulum systems, aiming to achieve better performance and robustness compared to integer-order control [4–7]. Several advancements in control strategies, stability analysis, and optimization methods for fractional-order controllers within the context of the IP-C system have been achieved. Prior works have primarily focalized on commensurate order systems, with notable contributions addressing stability concerns [8–10]. However, non-commensurate systems present a challenge, and recent approaches propose innovative methods for stability analysis in the frequency domain, such as the argument principle [11–14]. These methods enable the asymptotic stability analysis of non-commensurate systems described by state-space models with different fractional orders of derivatives of the state variables. To design fractional-order controllers ensuring stability, the argument principle variation of a rational function should tend to zero [11]. Moreover, the control design problem becomes multi-objective, aiming to simultaneously minimize the variation of the argument principle, integral of absolute error (IAE), and overshoot (M_p). To address this complex optimization problem, various approaches have been investigated, including classical methods extended for fractional systems, artificial intelligence-based techniques [15, 16],

and meta-heuristic approaches [17, 18]. Meta-heuristic methods, inspired by natural phenomena, offer promising solutions for optimizing the parameters of fractional-order controllers. Among these methods, particle swarm optimization (PSO) stands out as a stochastic heuristic algorithm that mimics the behaviour of species living in swarms [19–21]. Multi-objective PSO (MOPSO) algorithms, integrating the concept of Pareto optimality, have been applied to control design problems, providing a set of optimal parameters for fractional controllers [22–26].

1.2 | Research gap

The existing literature primarily focalize on systems with commensurate order, leaving a notable gap in the availability of analytical methods for investigating the stability of non-commensurate order systems. Despite a recent proposal for an innovative approach, grounded in the argument principle, to study stability in the frequency domain, it is underscored that no analytical methods currently exist for assessing stability in non-commensurate systems. The introduction of fractional-order control for linear time-invariant (LTI) systems adds a layer of intricacy, particularly in attaining specific performance objectives. The challenge lies in crafting controllers that ensure stability while simultaneously meeting diverse performance criteria. Specifically in the context of controlling an IP-C system, the importance of adopting a multi-objective optimization approach is emphasized. This necessity arises from the simultaneous consideration of three pivotal objectives: the variation of the argument principle, IAE, and M_p. This highlights the intricate nature of crafting controllers that can adeptly meet a diverse array of performance criteria. Furthermore, the paper suggests the essentiality of integrating meta-heuristic methods such as PSO to confront the complex optimization challenges ingrained in the design of fractional-order controllers.

1.3 | Motivation

The inspiration behind this research stems from the imperative to tackle significant hurdles in controlling an IP-C system, notorious for its inherent instability and non-linearity. Traditional control methods have been utilized, but their efficacy in consistently achieving satisfactory performance in the dynamic and complex IP-C system is questioned. The growing interest in fractional-order control techniques, as outlined in the [6, 27–29], arises from their potential to provide superior performance and robustness compared to conventional integer-order control methods. The unique challenge of determining unknown parameters in fractional controllers, especially in the non-commensurate order case, adds a layer of complexity. The motivation for this work is to contribute innovative solutions to these challenges by proposing a novel approach based on the argument principle in the frequency domain for the stability analysis of non-commensurate systems. The main focus of this endeavour centres on the strategic use of MOPSO to grapple with the intricacies of designing fractional-order controllers for the IP-C system. The ultimate goal is to seamlessly integrate theoretical advancements with practical applications and thereby contribute to the advancement of control strategies in dynamic systems.

1.4 | Contribution

Our present work brings several notable contributions to the field of control systems, particularly in the context of the IP-C system:

1.4.1 | The use of stability analysis for non-commensurate systems

The paper proposes a novel approach based on the argument principle in the frequency domain for the stability analysis of non-commensurate systems. This innovative method, as presented in [11, 12, 30], addresses a significant gap in the literature where stability analyses have primarily focused on commensurate order systems. The contribution lies in providing a theoretical framework for understanding and ensuring stability in non-commensurate fractional-order systems.

1.4.2 | Multi-objective optimization for fractional controllers

This work introduces a multi-objective optimization problem in the design of fractional-order controllers, with objectives including the variation of the argument principle, IAE, and M_p. This contribution advances the field by framing the control design problem as a multi-objective optimization task and proposes the use of meta-heuristic methods, specifically MOPSO, to address these conflicting objectives. The introduction of a MOPSO algorithm based on the Pareto principle, to our humble mind, is a key contribution. This algorithm is employed to compute the parameters of both the MOIF and MOPIF controllers. The integration of a meta-heuristic optimization approach contributes to the efficient determination of optimal control parameters considering multiple conflicting objectives.

1.4.3 | Development of fractional control laws

This paper proposes two controllers fractional order with state feedbacks, namely the MOIF order $u(t) = k_i I^{\alpha} e(t) + K_x x(t)$ and the MOPIF controller, where a proportional gain is added in parallel to the fractional integral part of the first controller $[u(t) = (k_p + k_i I^{\alpha}) e(t) + K_x x(t)]$. The challenge is then, to design the parameters K_x, k_p, k_i, and the non-integer order (α) for both controllers so as to best fulfil the requirements and desired performances and ensure the controllers efficiency.

1.4.4 | Simulation and experimental implementation and validation

The simulation of the non-linear model of the IP-C system constitutes a crucial step in this study, aiming to illustrate the similarity of its results with experimental results. This approach also allows the evaluation of robustness of the proposed controls in the face of disturbances and a 40% variation in the cart's mass. A comprehensive comparative study of the proposed controllers is also undertaken, comparing their performances to those of PID controllers and FOPID controller. The objective of this comparison is to highlight the significant advantages of the proposed controls. The next stage of the work is the experimental implementation of these two controllers on an IP-C system. The achieved experimental tests practically emphasize the chosen and developed approach. Additionally, we compare the results obtained from these experiments with those from a previous study [6], where a FOC was utilized. Notably, our comparison reveals substantial enhancements in key performance elements, including a notable reduction in overshoot (M_p), minimized static error ($\varepsilon(x)$), and an improved control mean value ($\bar{U}_m$). This comparative analysis highlights tangible advancements achieved through the implementation of the proposed fractional-order control laws in contrast to the use of a conventional FOC controller.

1.5 | Organization

The paper is outlined as follows: main generalities and reviews on fractional calculus are given in Section 2. Section 3 addresses the stability of the fractional order systems. The optimization based control design problem is stated and formulated in Section 4. The applied PSO algorithm is briefly described in Section 5. Section 6 is devoted to the description of the inverted pendulum-cart system and the discussion of the obtained simulation and experimental results. Finally, a conclusion summarizes the paper contribution in Section 7.

2 | STABILITY OF FRACTIONAL ORDER SYSTEM

A continuous time linear system of fractional orders is described by the homogeneous state Equation [11, 12]:

$$ {}_0D_t^{\bar{\alpha}} x(t) = A\, x(t) \tag{1} $$

with

$$ x(t) = \begin{bmatrix} x_1(t) \\ \vdots \\ x_n(t) \end{bmatrix}, {}_0D_t^{\bar{\alpha}} x(t) = \begin{bmatrix} {}_0D_t^{\alpha_1} x_1(t) \\ \vdots \\ {}_0D_t^{\alpha_n} x_n(t) \end{bmatrix} \tag{2} $$

$$ A = \begin{bmatrix} A_{11} & \cdots & A_{1n} \\ \vdots & \ddots & \vdots \\ A_{n1} & \cdots & A_{nn} \end{bmatrix} \tag{3} $$

and $x_k(t) \in \Re^{n_k}$, $k = 1, \ldots, n, A_{kr} \in \Re^{n_k \times n_r} (k, r = 1 \ldots n)$.

${}_0D^{\bar{\alpha}} x(t)$ is the fractional derivative of non-integer order α of $x(t)$ according to the Caputo definition of the derivative, given as follows [31]:

$$ {}_0D_t^{\alpha_k} x_i(t) = \frac{1}{\Gamma(p_k - \alpha_k)} \int_0^t \frac{x_i^{(p_k)}(\tau) \mathrm{d}\tau}{(t-\tau)^{\alpha_k} - p_k + 1} \tag{4} $$

Γ is Euler's gamma function and p_k is the positive integer [32]. The Laplace transform of ${}_0D_t^{\bar{\alpha}} x(t)$ with zero initial conditions is defined by:

$$ \mathfrak{L}\{{}_0D_t^{\bar{\alpha}} x(t)\} = \begin{bmatrix} s^{\alpha_1} X_1(s) \\ \vdots \\ s^{\alpha_n} X_n(s) \end{bmatrix} \tag{5} $$

where $X_k(s)$ is the Laplace transform of $x_k(t)$ with $k = 1, \ldots n$.

The characteristic matrix of Equation (1) is given as follows:

$$ H(s) = \begin{bmatrix} I_{n_1} s^{\alpha_1} - A_{11} & \cdots & -A_{1n} \\ -A_{21} & \vdots & -A_{2n} \\ \vdots & \ddots & \vdots \\ A_{n1} & \cdots & I_{n_n} s^{\alpha_n} - A_{nn} \end{bmatrix} \tag{6} $$

The characteristic polynomial of A is:

$$ \omega(s) = \det(H(s)) \tag{7} $$

$\omega(s)$ is a polynomial of fractional degree δ given by:

$$ \delta = n_1\alpha_1 + n_2\alpha_2 + \cdots + n_n\alpha_n \tag{8} $$

For studying the stability of system (1), three cases are considered in [11]: the commensurate order, the rational order and a non-commensurate order.

2.1 | Stability of a commensurate-order system

The fractional-order system is commensurate order if there exists a real number $\alpha > 0$, such that:

$$ \alpha_i = K_i \alpha, \qquad i = 1, \ldots, n. \quad K_i \in Z_+ \tag{9} $$

by taking:

$$ \lambda = s^{\alpha}, \tag{10} $$

Equations (6) and (7) take the following form:

$$ H(\lambda) = I(\lambda) - A \tag{11} $$

with

$$ I(\lambda) = \begin{bmatrix} I_{n_1}\lambda^{K_1} & 0 & \cdots & 0 \\ 0 & I_{n_2}\lambda^{K_2} & \cdots & 0 \\ \vdots & \vdots & \ddots & \vdots \\ 0 & 0 & \cdots & I_{n_n}\lambda^{K_n} \end{bmatrix} \tag{12} $$

and the characteristic polynomial $\omega(\lambda)$ is an integer order polynomial given by:

$$\omega(\lambda) = \det(H(\lambda)) = \lambda^p + a_{p-1}\lambda^{p-1} + \cdots + a_0 \quad (13)$$

where $a_k \quad (k = 0, 1, \ldots, p-1)$ are a real numbers and

$$p = \sum_{i=1}^{n} n_i k_i \quad (14)$$

The linear fractional-order system (1) is stable if and only if the condition of Matignon

$$|\arg(\lambda_i)| > \alpha\frac{\pi}{2} \quad (15)$$

is satisfied for all roots λ_i of the polynomial $w(\lambda)$ given by Equation (13) and it is demonstrated in [12] and [33] that the polynomial $w(s)$ is unstable for all $\alpha > 2$.

2.2 | Stability of non-commensurate-order system

For this kind of system, the frequency domain method is applied. This method is proposed in [11] for asymptotic stability analysis of continuous time linear systems.

Theorem 1 [11]. *System (1), with non-commensurate fractional order is asymptotically stable if and only if:*

$$\Delta_{\omega\in(-\infty,+\infty)}Arg[\psi(j\omega)] = 0 \quad (16)$$

with

$$\psi(s) = \frac{\omega(s)}{\omega_r(s)} = \frac{det(I(s) - A)}{\omega_r(s)} \quad (17)$$

where $\omega_r(s)$ is the reference asymptotically stable polynomial of fractional degree with:

$$\omega_r(s) = (s + c)^\delta, \quad c > 0 \quad (18)$$

and $\psi(j\omega) = \psi(s)$ for $s = j\omega$. Equation (16) holds, means it that the plot of $\psi(j\omega)$ does not encircle or cross the origin of complex plane (Nyquist plots) as ω runs from $-\infty$ to $+\infty$. From Equations (16) and (17) we have

$$\psi(\infty) = \lim_{\omega\to+\infty}\psi(j\omega) = 1 \quad (19)$$

and

$$\psi(0) = \frac{\det(-A)}{c^\delta} \quad (20)$$

Lemma 1 [11]. *if $det(-A) \leq 0$, then the fractional order system (1) is unstable.*

Before applying Theorem 1 to study the stability of system (1), we have to verify the condition given by Lemma 1. Then if this condition is satisfied we deduce directly that system (1) is unstable.

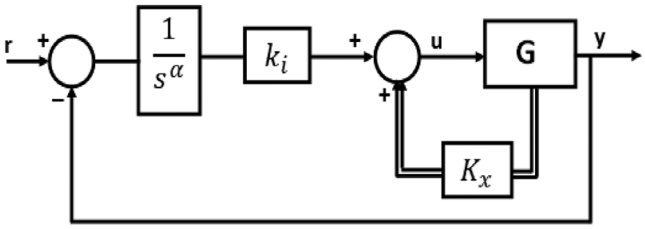

FIGURE 1 Block diagram of MOIF control.

3 | PROBLEM FORMULATION

3.1 | Fractional order integral with a state feedback control

In this section, a MOIF controller with state feedback is introduced (Figure 1).

In this study, a control system based on fractional calculus and state feedback. The system under consideration is represented by a (SISO) system denoted as G. The control law governing the system is expressed as follows:

$$u(t) = k_i I^\alpha(e(t)) + K_x x(t) \quad (21)$$

where k_i denotes the integral gain, α represents the fractional order of the integrator with $0 < \alpha < 1$, and K_x is the proportional gain vector associated with the state feedback ($K_x = [K_{x_1}, K_{x_2}, \ldots K_{x_n}]$). The state space model describing the closed-loop system is as follows:

$$\begin{bmatrix} \dot{x} \\ D^\alpha x_r \end{bmatrix} = \begin{bmatrix} (A + BK_x) & Bk_i \\ -C & 0 \end{bmatrix}\begin{bmatrix} x \\ x_r \end{bmatrix} + \begin{bmatrix} 0 \\ 1 \end{bmatrix} r \quad (22)$$

We notice that $\begin{bmatrix} (A + BK_x) & Bk_i \\ -C & 0 \end{bmatrix}$ takes the same form as Equation (3), allowing us to employ Theorem 1 to analyse the stability of system. The characteristic matrix corresponding to Equation (22) is:

$$H_1(s) = \begin{bmatrix} I_{11}s - [A + BK_x] & -Bk_i \\ -C & I_{22}s^\alpha - 0 \end{bmatrix} \quad (23)$$

and according to Theorem 1 we have:

$$\psi_1(s) = \frac{\det(H_1(s))}{(s + c)^\delta} \quad (24)$$

In order to meet the stability requirements given by Theorem 1 and simultaneously minimize both the error and overshoot, the control law parameters, specifically α, k_i, and K_x are determined using a Pareto-based multi-objective optimization approach. This optimization method employs the PSO.

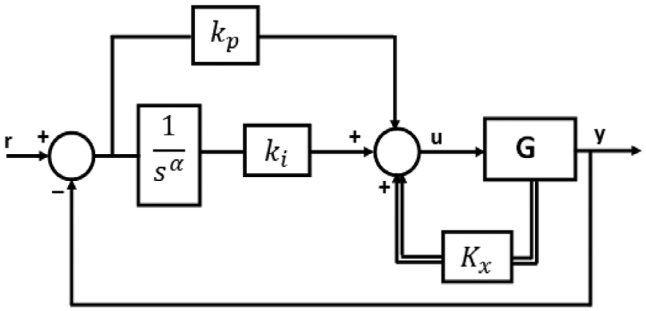

FIGURE 2 Block diagram of MOPIF control.

3.2 | Fractional order proportional integral with a state feedback control

In this section, a MOPIF controller with state feedback is introduced. In order to increase the capabilities of the controller defined by Equation (21), a PI^α controller is used as depicted in Figure 2. The objective of this modification is to harness the benefits offered by fractional calculus, by combining both proportional and fractional integral components. This hybrid approach provides better adaptability to complex and dynamic systems, such as an inverted pendulum.

the corresponding control law is defined by:

$$u(t) = k_p e(t) + k_i I^\alpha e(t) + K_x x(t) \tag{25}$$

The determination of parameters k_p, k_i, K_x and α adheres to a similar formulation as presented in Equations (22)–(24), employing the PSO multi-objective optimization algorithm. This methodology ensures an iterative exploration of the parameter space to achieve optimal values, considering multiple objectives simultaneously.

The state representation of the closed-loop system is then given by:

$$\begin{bmatrix} \dot{x} \\ D^\alpha x_r \end{bmatrix} = \begin{bmatrix} (A + BK_x - k_p BC) & Bk_i \\ -C & 0 \end{bmatrix} \begin{bmatrix} x \\ x_r \end{bmatrix} + \begin{bmatrix} Bk_p \\ 1 \end{bmatrix} r \tag{26}$$

The characteristic matrix corresponding to Equation (26) is:

$$H_2(s) = \begin{bmatrix} I_{11}s - [A + BK_x - k_p BC] & -Bk_i \\ -C & I_{22}s^\alpha - 0 \end{bmatrix} \tag{27}$$

and according to Theorem 1 we have:

$$\psi_2(s) = \frac{det(H_2(s))}{(s+\epsilon)^\delta} \tag{28}$$

4 | CONTROLLER DESIGN

To determine the controller parameters given by Equations (21) and (25), using a PSO multi-objective optimization approach, the parameters under certain constraints must be specified. The two controllers, i.e. MOIF and MOPIF, involve different sets of parameters: • For MOIF controller:

$$X = (X_1, X_2, X_3) = (\alpha, k_i, K_x) \tag{29}$$

• For MOPIF controller:

$$X = (X_1, X_2, X_3, X_4) = (\alpha, k_p, k_i, K_x) \tag{30}$$

where α, k_p, k_i are scalars and K_x is a vector.

Finding the tuning of this controller gains given in Equations (29) and (30), can be established as multi-objective optimization problem includes three objective functions as:

$$\text{Minimize } f(X) = (f_1(X), f_2(X), f_3(X)) \tag{31}$$

Where:

$$\begin{aligned} f_1(X) &= M_p \\ f_2(X) &= \int_{t_0}^{\infty} |e(t)| dt \\ f_3(X) &= \psi(jw) \\ \text{with } & 0 < \alpha < 1 \end{aligned} \tag{32}$$

where $e(t)$ is the control error defined as $(e(t) = r(t) - y(t))$. f_1 is the overshoot (M_p) of the response to as step reference input, knowing that M_p is desired as low as possible, while the settling time t_r is desired to be of acceptable range.

f_2 is the integral absolute tracking error (e_{IAE}) defined as:

$$e_{IAE} = \int_{t_0}^{\infty} |r(t) - y(t)| dt \tag{33}$$

The election of IAE is because it is simple and leads to satisfactory control performance.

The function f_3 allows to satisfy the frequency domain stability condition given by Theorem 1. This ensures stability of the closed-loop system described by Equations (22) and (26) in the frequency domain.

Optimizing all three objectives simultaneously might not yield a unique solution. Instead, the goal is to obtain a set of solutions known as Pareto solutions. These solutions represent trade-offs among the conflicting objectives, allowing for a comprehensive understanding of the system's performance under various conditions.

The flowchart illustrating the proposed algorithm is presented in Figure 3.

5 | IP-C SYSTEM IMPLEMENTATION

In this section, the performance and effectiveness of the MOIF and MOPIF controllers proposed in Sections 3 and 4, are evaluated in an inverted pendulum-cart shown in Figure 4. The control of this system consists in the control of swing-up of inverted pendulum and in the control of cart moving on a track, via a DC motor attached at the end of the rail. Essentially, we control two variables, the pendulum angle θ and the cart position x. The latter is bounded by the rail length $x = \pm 0.4$ m. So,

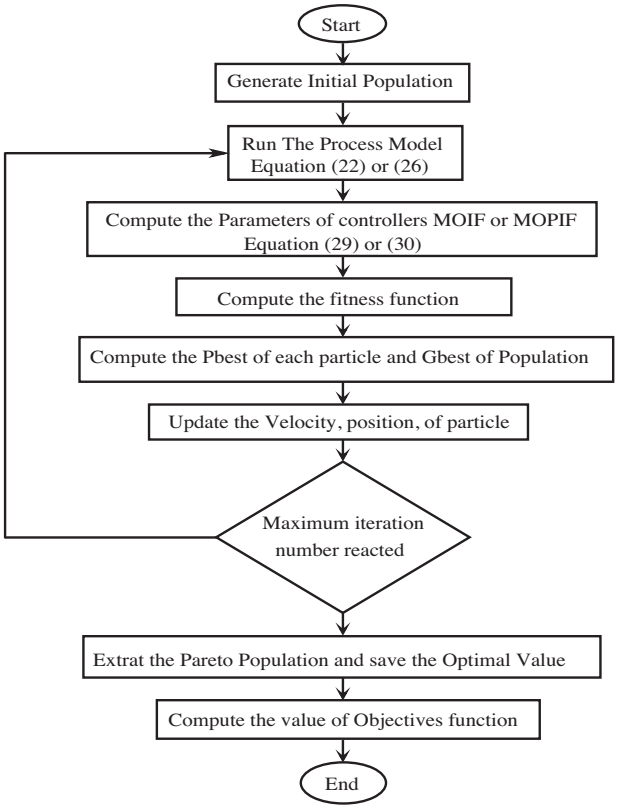

FIGURE 3 Flowchart of PSO multi-objective algorithm.

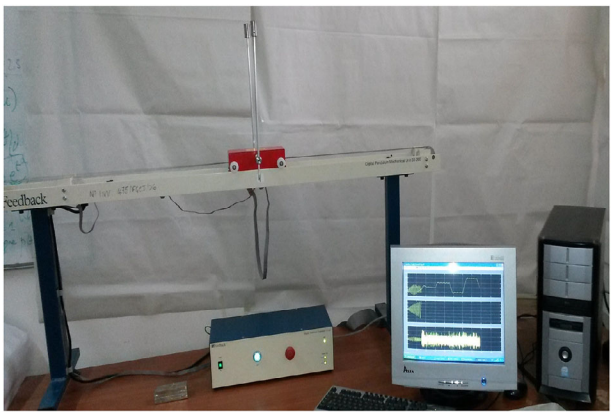

FIGURE 4 Pendulum-cart system.

the non linear model is linearized around the unstable equilibrium $\theta = 0$. The linear model of the IP-C can be modelled in the state space representation as follows [4]:

$$\begin{cases} \dot{x} = Ax + Bu & x(0) = x_0 \\ y = Cx \end{cases} \tag{34}$$

where x is the state vector as follows:

$$x = \begin{bmatrix} x_p & \dot{x}_p & \theta & \dot{\theta} \end{bmatrix}^T \tag{35}$$

In this expression x_p is the cart position, $\dot{x}_p$ is its velocity, θ is the pendulum angle and $\dot{\theta}$ is the angular velocity. Besides, we have:

$$A = \begin{bmatrix} 0 & 1 & 0 & 0 \\ 0 & \frac{-bN}{bN - m^2l^2} & \frac{-gm^2l^2}{bN - m^2l^2} & \frac{mld}{bN - m^2l^2} \\ 0 & 0 & 0 & 1 \\ 0 & \frac{mlb}{bN - m^2l^2} & \frac{-mgl}{N} + \frac{m^3l^3g}{N(bN - m^2l^2)} & \frac{-d}{N} + \frac{m^2l^2d}{N(bN - m^2l^2)} \end{bmatrix}$$

$$B = \begin{bmatrix} 0 \\ \frac{N}{bN - m^2l^2} \\ 0 \\ \frac{-ml}{bN - m^2l^2} \end{bmatrix}$$

$$C = \begin{bmatrix} 1 & 0 & 0 & 0 \\ 0 & 0 & 1 & 0 \end{bmatrix} \tag{36}$$

Numerical values of all the parameters of IP-C System are given in Table 1, and the numerical values of A and B are:

$$A = \begin{bmatrix} 0 & 1 & 0 & 0 \\ 0 & -2.1\,10^{-5} & -0.5339 & 0.0045 \\ 0 & 0 & 0 & 1 \\ 0 & 4.5\,10^{-5} & 22.2449 & -0.189 \end{bmatrix}, \tag{37}$$

$$B = \begin{bmatrix} 0 \\ 0.4218 \\ 0 \\ -0.970 \end{bmatrix}$$

the poles of linear model (37) are:

TABLE 1 Parameters of IP-C system.

Parameter	Notation	Value
Cart mass	M	2.3 kg
Pendulum mass	m	0.2 kg
Pendulum half length	l	0.36 m
Moment of inertia	J	0.099 kg/m^2
Friction coefficient of the cart wheels	b	0.05 kg m^2/s
Rotation friction of the pendulum	d	0.005 kg m^2/s
Acceleration constant	g	9.81 m/s^2

TABLE 2 Performance criteria of the (MOIF, MOPIF, PID, FOPID controllers) obtained by simulation.

Controllers	M_p	t_r (s)	$\varepsilon(x)$
MOPIF	10	4.95	0, 0047
MOIF	12,2	7,8	0, 0052
PID	57	14,58	0, 0048
FOPID	35	8,5	0, 003

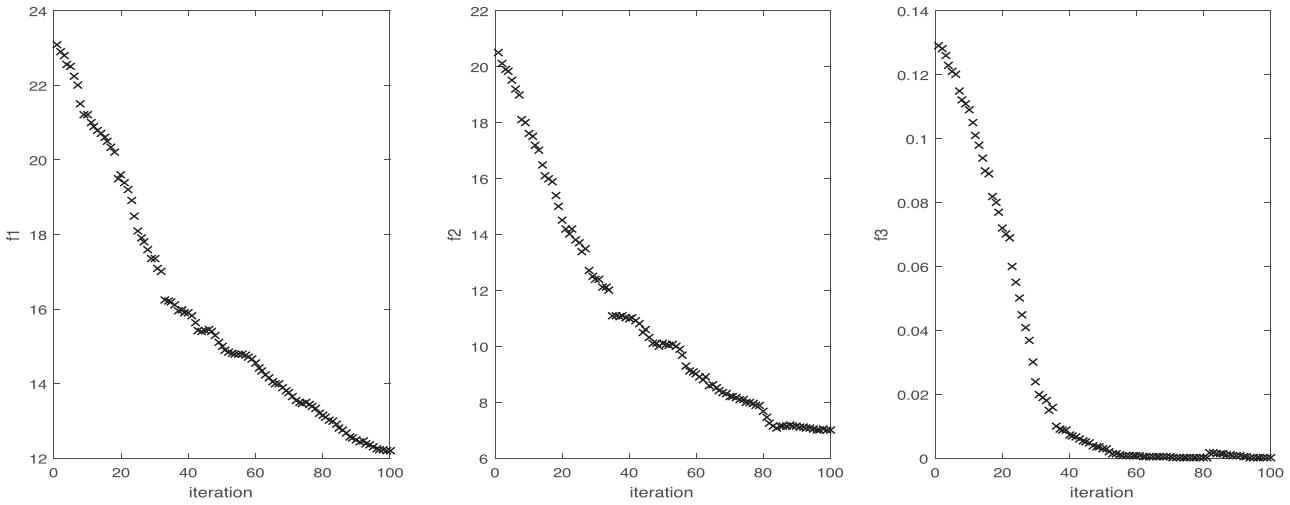

FIGURE 5 Convergence of f1,f2, and f3 for MOIPF.

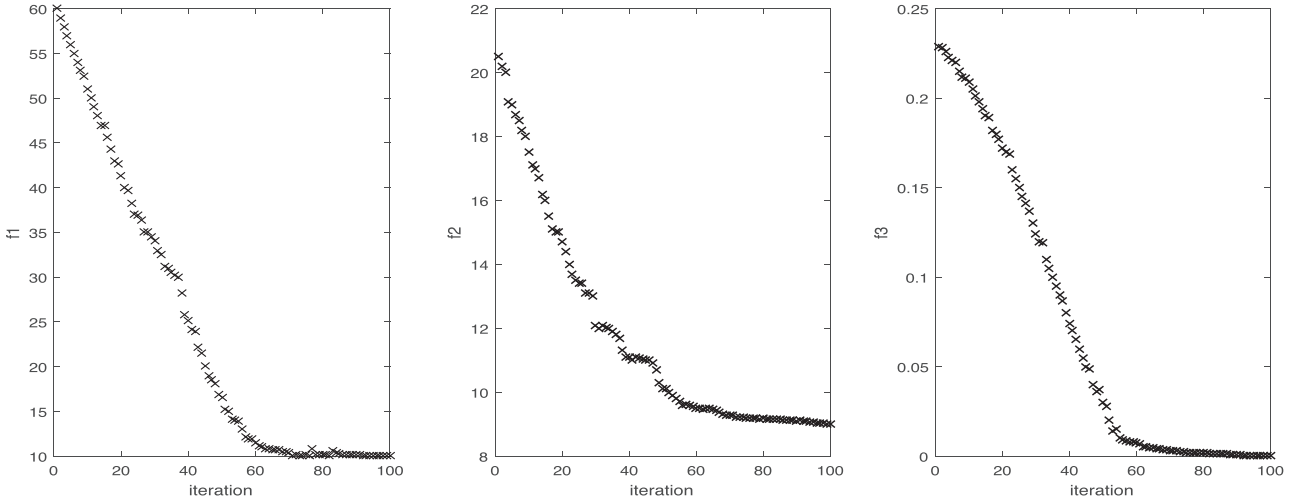

FIGURE 6 Convergence of f1,f2, and f3 for MOIPF.

$p_1 = 0, p_2 = 0, p_3 = 4.06229$, and $p_4 = -4.8119$, thus the system is unstable.

5.1 | Simulation and experimental results

The controllers MOIF and MOPIF described in Section 3 are implemented to test their stability and reference tracking capabilities system. The MOPSO parameters are given in Table 2 as:

The MOPSO algorithm is used to searching and optimizing the MOIF and MOPIF controllers parameters, namely respectively

(α, k_i, K_x) and (α, k_p, k_i, K_x).

Since the order of state matrix A of the IP-C system is $n = 4$, then the vector gain K_x has the following form:

$$K_x = \begin{bmatrix} K_{x_1} & K_{x_2} & K_{x_3} & K_{x_4} \end{bmatrix} \tag{38}$$

Hence, each particle has six members $(\alpha, k_i, K_{x1}, K_{x2}, K_{x_3}, K_{x4})$ attribute for MOIF controller and seven member

$(\alpha, k_p, K_i, K_{x1}, K_{x2}, K_{x_3}, K_{x4})$ attributed for MOPIF controller, Then the dimensions of that population are $6n$ and $7n$ for MOIF and MOPIF controllers, respectively. The optimal parameters of the MOIF controller are:

$$\begin{cases} \alpha = 0.18 \\ k_i = 3.8 \\ K_x = \begin{bmatrix} 2.01 & 17.12 & 110.00 & 14.03 \end{bmatrix} \end{cases} \tag{39}$$

and those of the MOPIF controller are:

$$\begin{cases} \alpha = 0.17 \\ k_i = 2.97 \\ k_p = 4.5 \\ K_x = \begin{bmatrix} 0.43 & 9.58 & 78.6 & 7.36 \end{bmatrix} \end{cases} \tag{40}$$

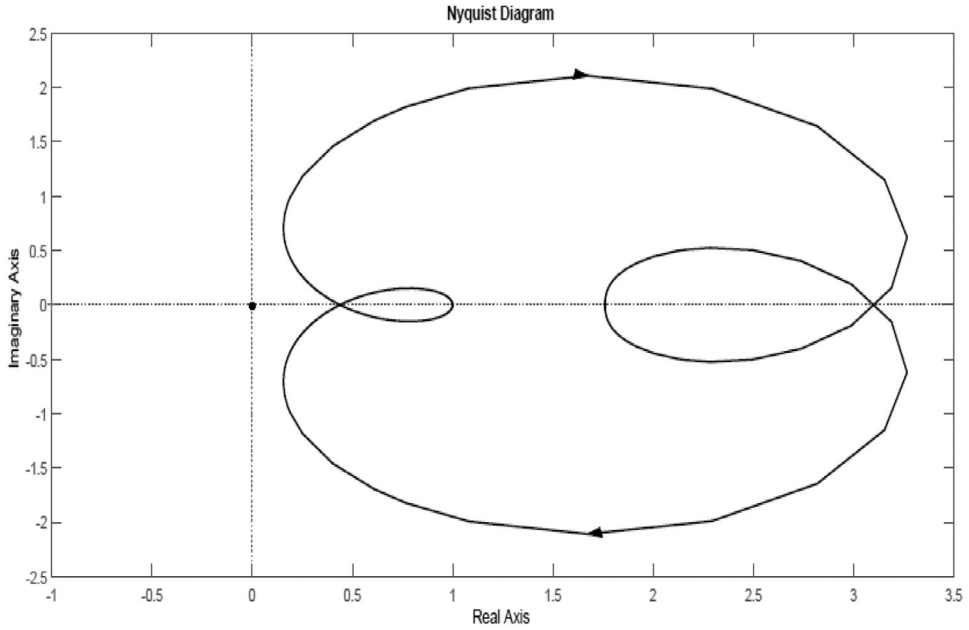

FIGURE 7 Nyquist MOIF.

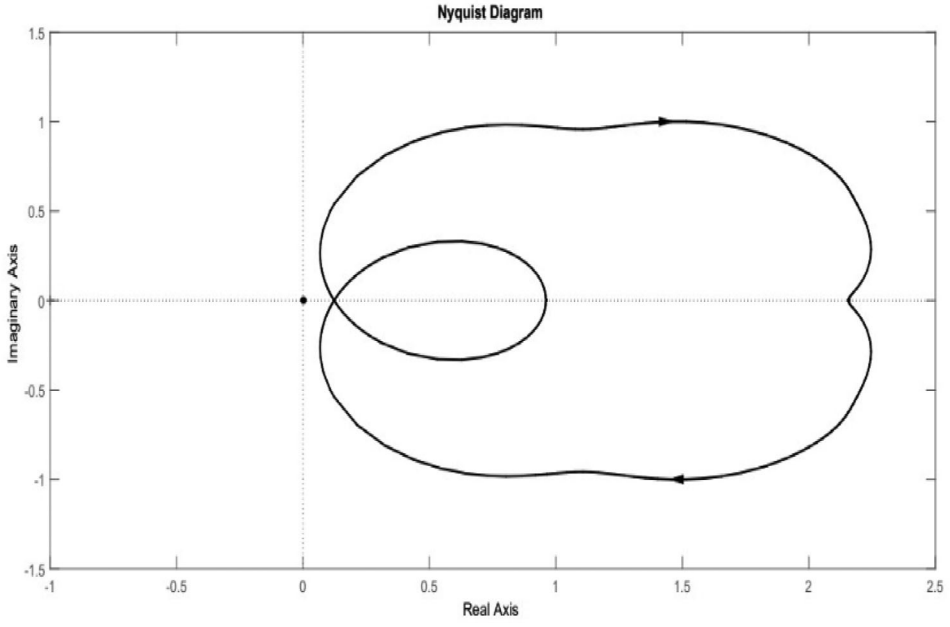

FIGURE 8 Nyquist MOPIF.

by substituting the parameters of controllers MOIF and MOPIF and into Equations (23) and (27), we obtain:

$$H_1(s) = \begin{bmatrix} s & -1 & 0 & 0 & 0 \\ -0.62 & s-4.76 & -33.92 & -4.38 & -1.18 \\ 0 & 0 & s & -1 & 0 \\ 1.35 & 10.25 & 51.86 & s+9.61 & 2.55 \\ 1 & 0 & 0 & 0 & s^{0.18} \end{bmatrix} \quad (41)$$

$$H_2(s) = \begin{bmatrix} s & -1 & 0 & 0 & 0 \\ 1.27 & s-2.41 & -24.02 & -2.30 & -0.92 \\ 0 & 0 & s & -1 & 0 \\ -2.73 & 5.19 & 30.56 & s+5.13 & 1.99 \\ 1 & 0 & 0 & 0 & s^{0.17} \end{bmatrix} \quad (42)$$

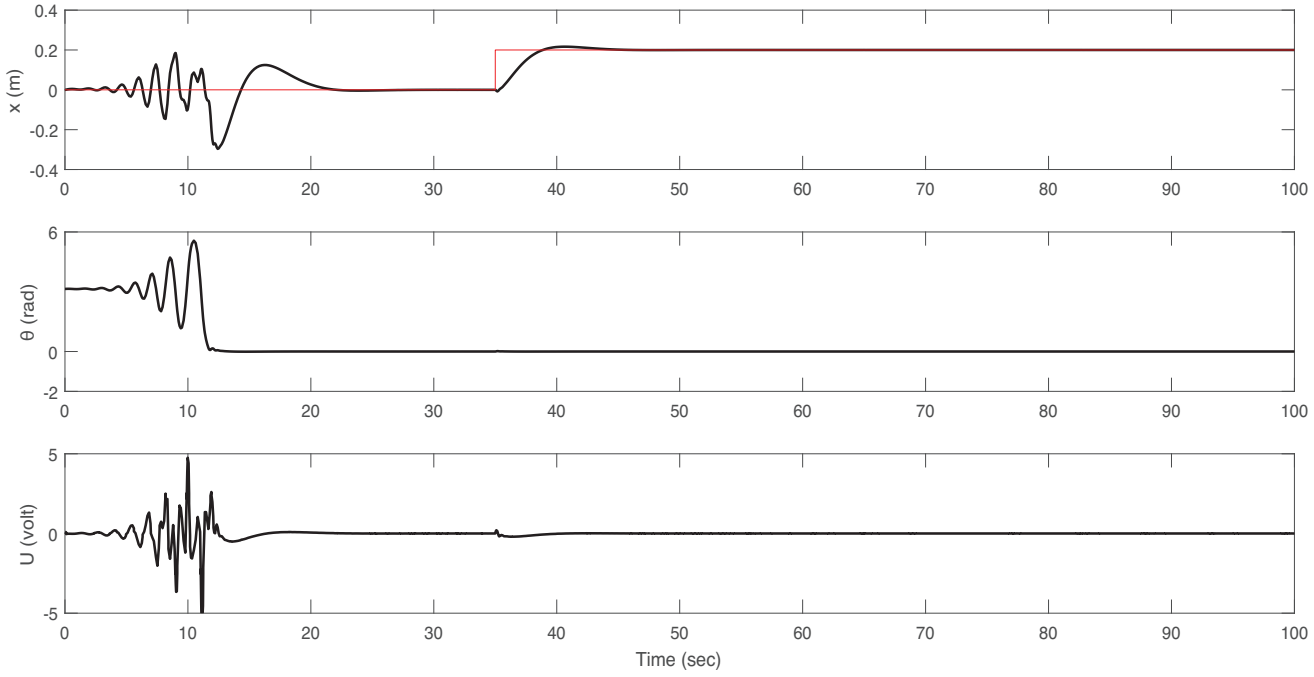

FIGURE 9 Simulation results of MOIF controller.

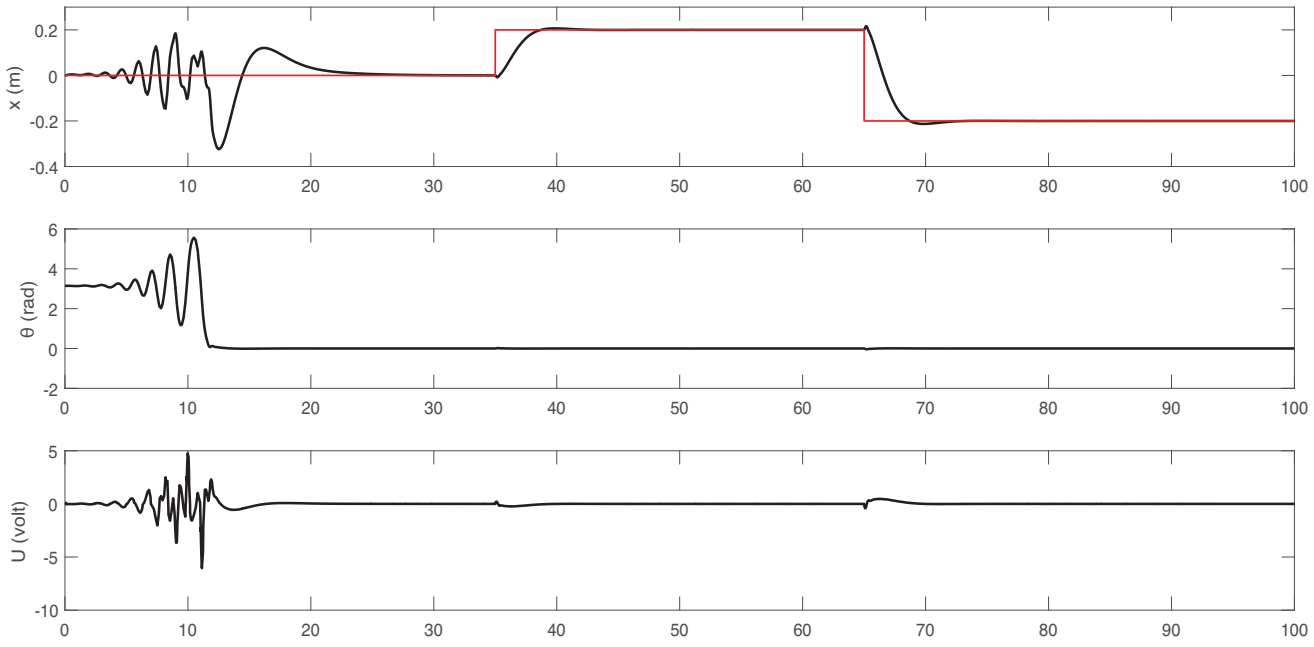

FIGURE 10 Simulation results of MOPIF controller.

According to Theorem 1, we have:

$$\psi_1(s) = \frac{\det(H_1)}{(s+3)^{2.18}} \tag{43}$$

and

$$\psi_2(s) = \frac{\det(H_2)}{(s+3)^{2.17}} \tag{44}$$

The result and the convergence of the three objective functions given by Equation 32 are given by Figures 5 and 6 for MOIF and MOPIF controllers.

The Nyquist plots of function (41) and (42) are given by Figure 7 and 8 respectively.

Figures 7 and 8 show that the plots of function (41) and (42) do not encircle the origin of the complex plane. Hence, the fractional order system with MOIF and MOPIF controllers are asymptotically stable. The controllers MOIF and MOPIF are

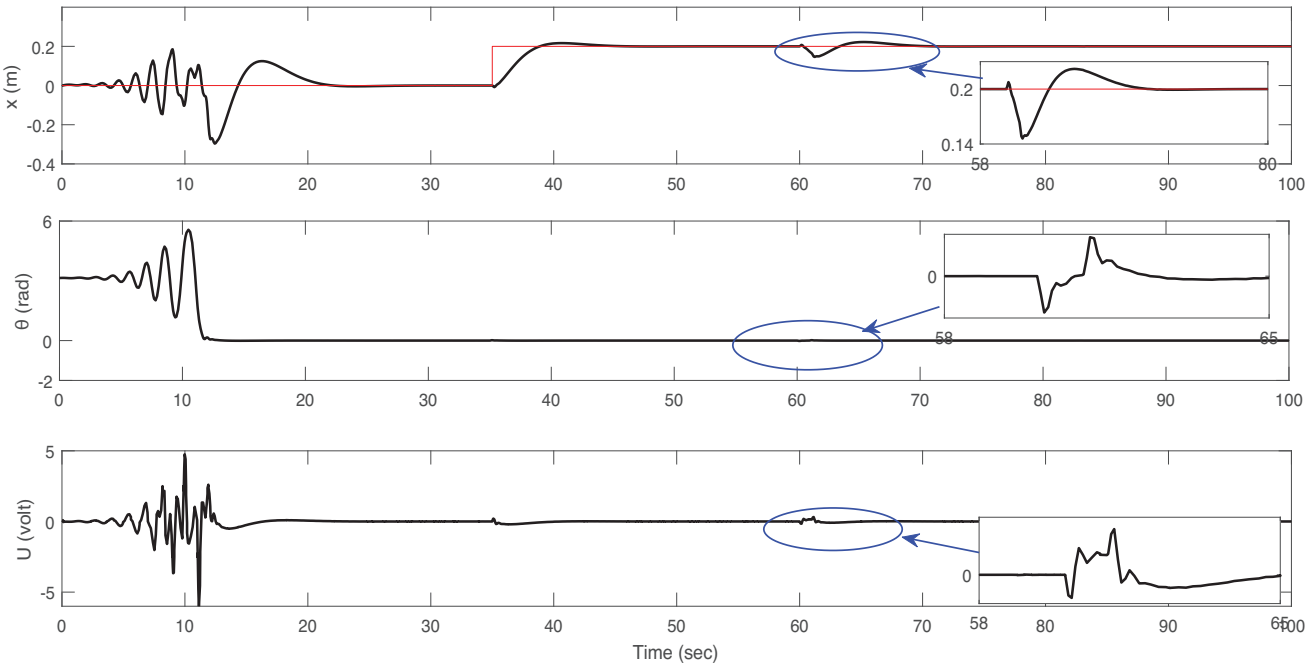

FIGURE 11 MOIF control result with impulse disturbance at $t = 60$ s.

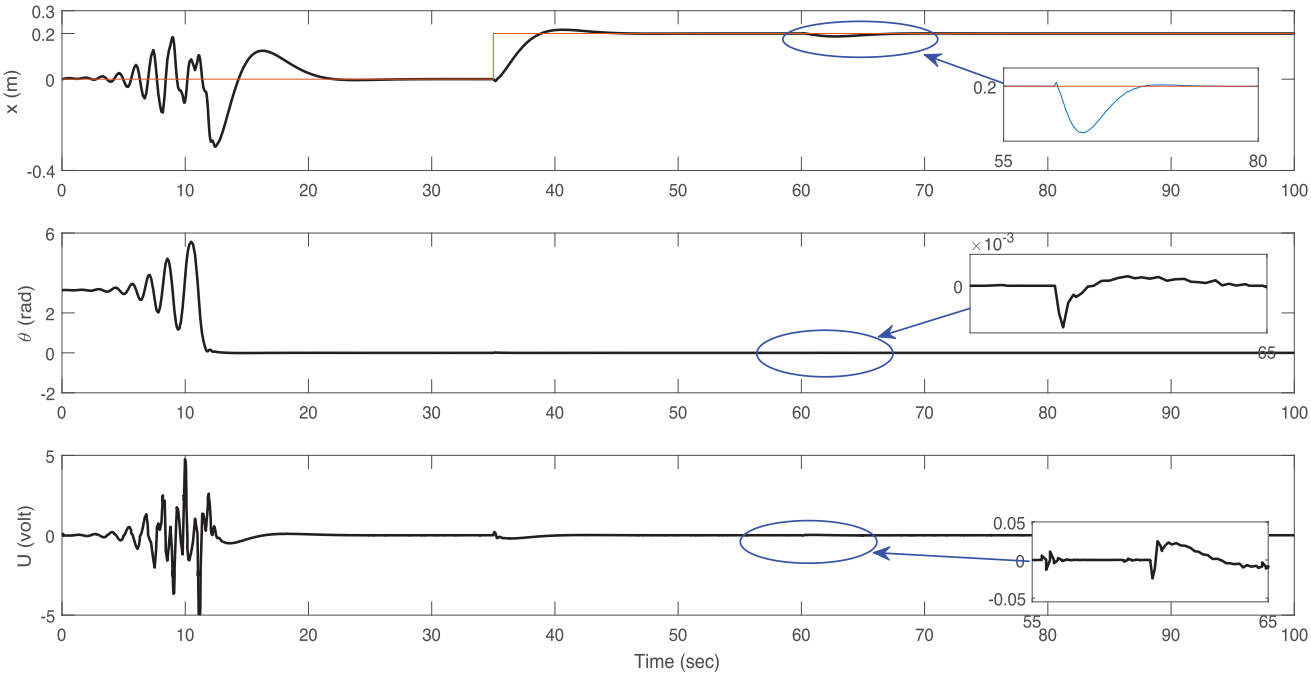

FIGURE 12 MOIF control result with step disturbance at $t = 60$ s.

simulated with success in the case of an the non-linear model of IP-C system.

The results are given by Figures 9 and 10. To assess the robustness of both controllers, MOIF and MOPIF, simulation runs are performed using the non-linear model of the IP-C system. The cases of an impulse and a step disturbances, and variations in the mass of the cart are investigated.

Figures 11–13 give the simulation results obtained with the MOIF controller in the case of an impulse disturbance, a step disturbance and a variation of 40% in the cart mass, respectively. Figures 14–16 illustrate the simulation results in the case of the MOPIF controller in response to the same disturbances. The simulation results given by Figures 11, 12, 14, and 15 show the dynamic behaviours of the MOIF and MOPIF controllers for diverse scenarios. These results highlight the capability of these controllers in handling disturbances. Furthermore, Figures 13 and 16 illustrate that, despite a significant 40% fluctuation in cart mass, stability reigns with a slight decrease in static error.

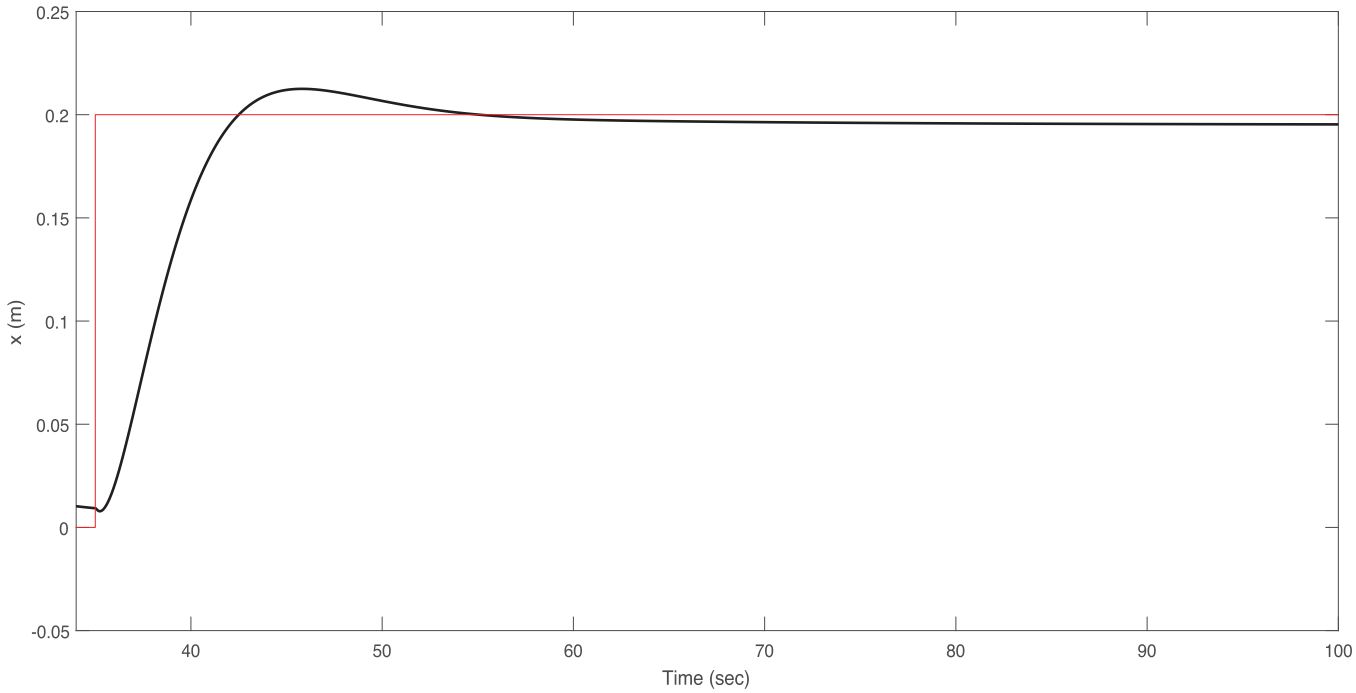

FIGURE 13 MOIF control result with 40% mass variation.

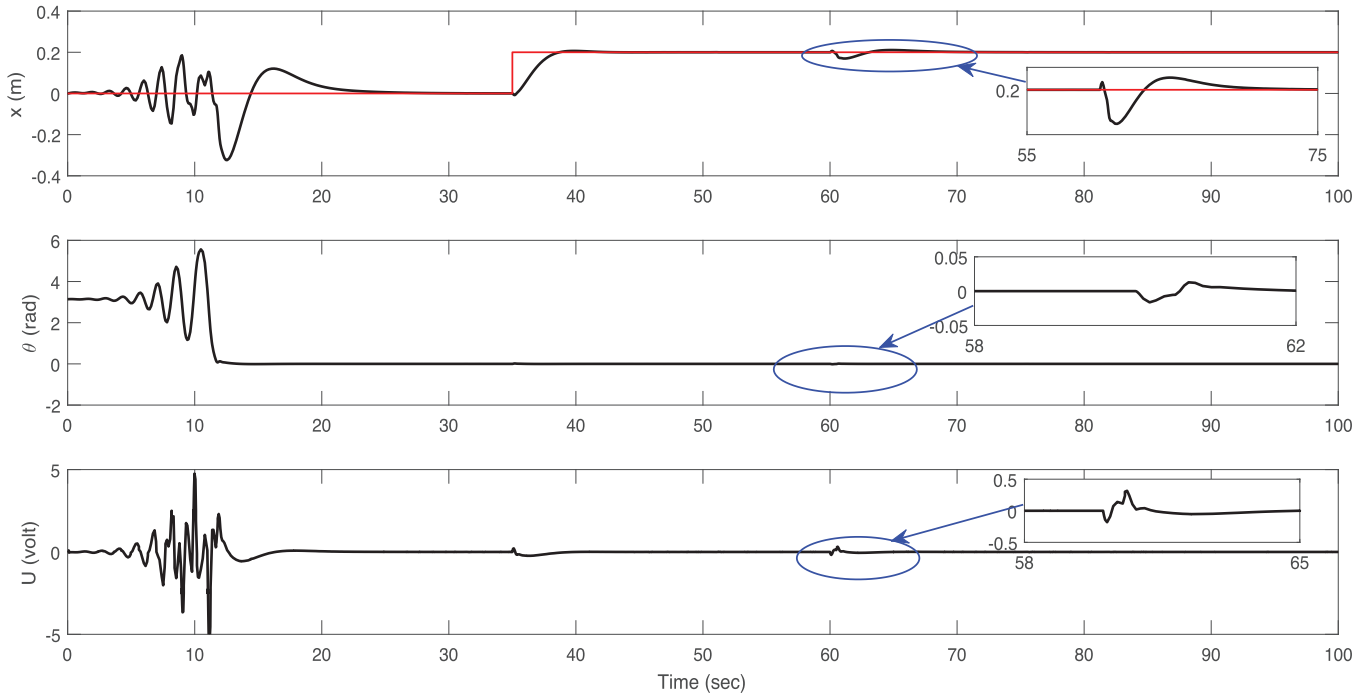

FIGURE 14 MOPIF control result with impulse disturbance at $t = 60$ s.

These results demonstrates the efficiency of the MOIF and MOPIF controllers.

The results of the proposed method are compared with those obtained by classical PID and fractional order FOPID controllers [34], using the same algorithm MOPSO employed to tuning the parameters of the MOIPF and MOIPF controllers. In Figure 17, simulation results from the four controllers (MOIPF, MOIF, PID, FOPID) are presented for set-point tracking. Figure 18 offers a closer look between the 35th and 60th seconds, providing a detailed illustration of the overshoot exhibited by each controller. The performance for all four controllers, including overshoots (M_p), settling times (t_r), and cart

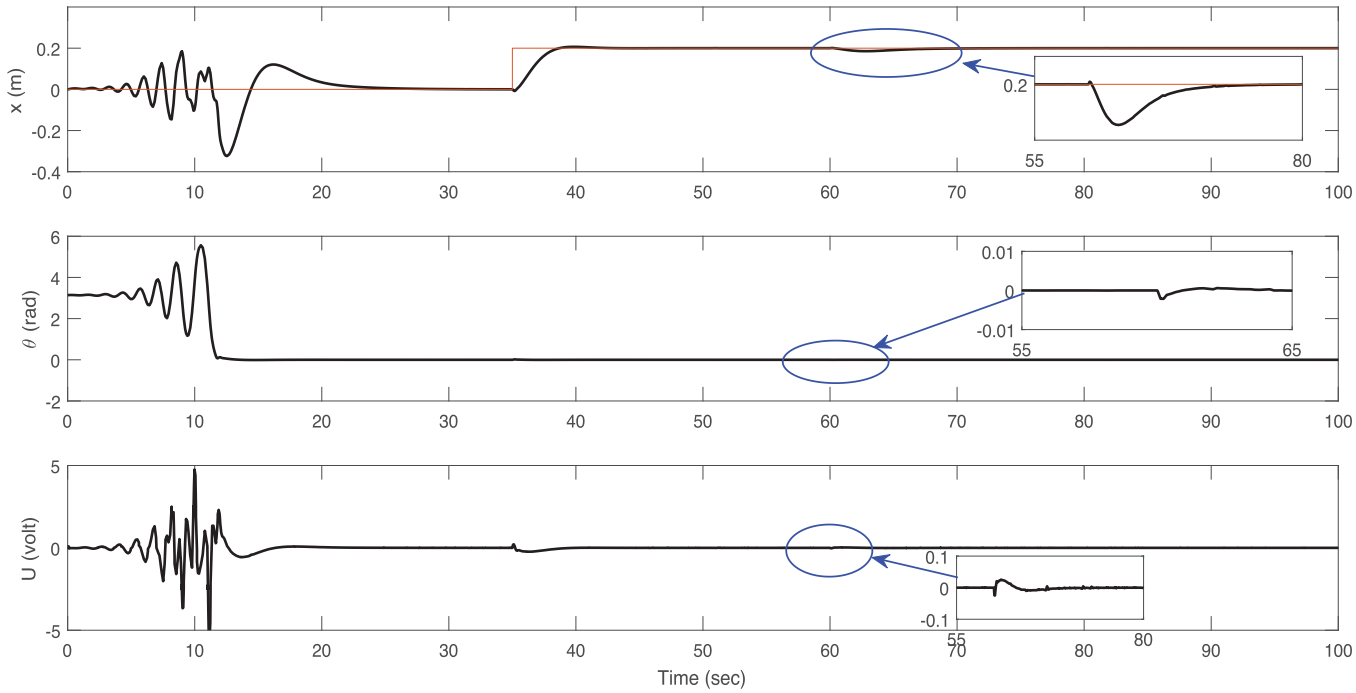

FIGURE 15 MOPIF control result with step disturbance at $t = 60$ s.

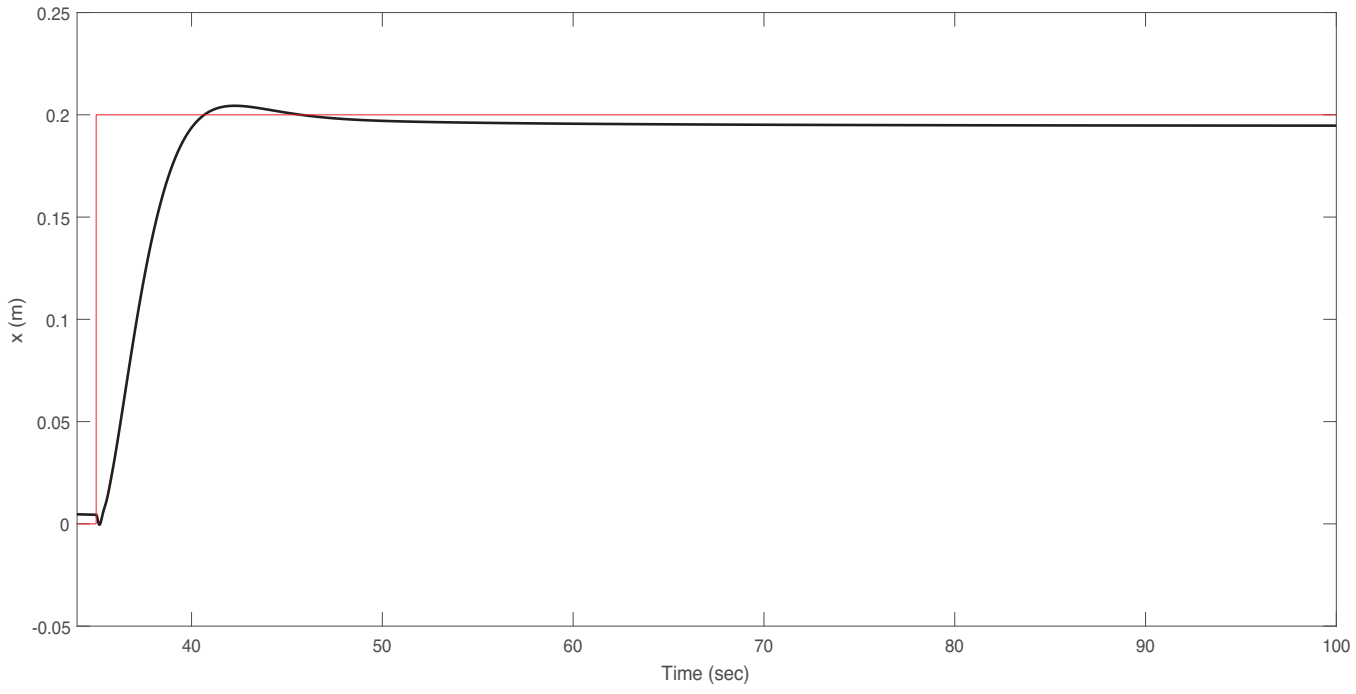

FIGURE 16 MOPIF control result with 40% mass variation.

tracking position errors $\varepsilon(x)$ are summarized in Table 2. A conclusion drawn from the table indicates that the position error values are nearly identical across all four controllers. However, the settling time values for MOIPF and MOIPF controllers are noticeably lower compared to PID and FOPID controllers. Furthermore, the overshoot values for MOIPF and MOIPF controllers is more better than those of the other controllers, indicating superior performance in this aspect.

And to demonstrate the effectiveness of this controllers, then they are implemented in IP-C system.

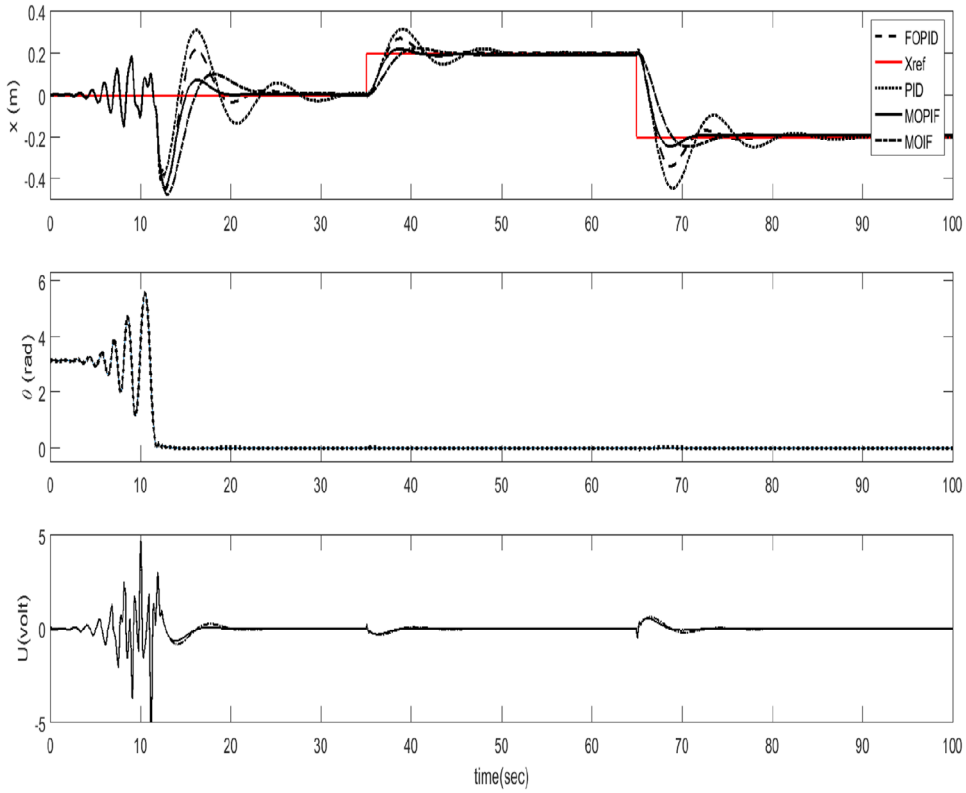

FIGURE 17 simulation results of PID-FOPID-MOIF-MOPIF controllers.

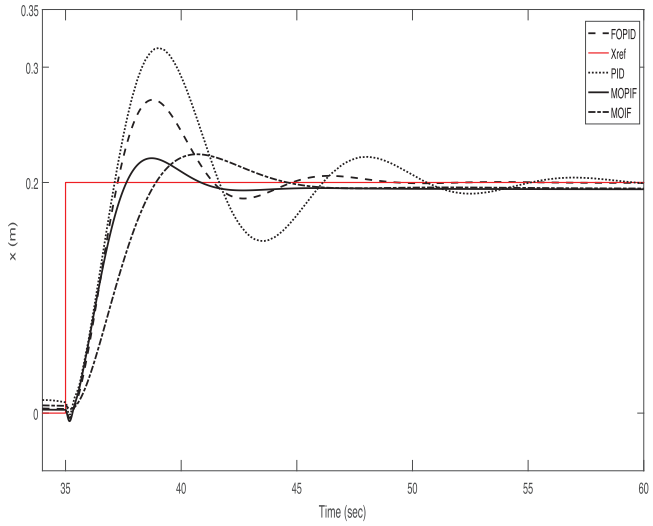

FIGURE 18 Focus on the x position of the four controllers between 35 and 60 s.

Figures 19 and 20 show the experimental results with the same value of parameters controllers given in Equations (37) and (38).

Once computed and simulated with the appropriate parameters according to Equations (37) and (38) given previously, the designed controllers MOIF and MOPIF are implemented on inverted pendulum-cart system. The sampling period is fixed at 0.001 s and the fractional orders operator's are approximated with the Oustaloup's method in frequency interval $[10^{-15}10^{+15}]$ with 15 cells.

TABLE 3 Performance criteria of the MOIF, MOPIF, and FOC controllers.

Controllers	M_p	t_r (s)	$\varepsilon(x)$	$\bar{U_m}$
MOIF	14	9	3.10^{-4}	0.1
MOPIF	4	4.15	1.10^{-4}	0.14
FOC	28.8	7	4.10^{-4}	0.1

At first, a swing up control is applied on the pendulum to reach the unstable vertical position ($\theta = 0$ or $\theta = \pi$). Once this position is reached, the designed controller keeps the pendulum at this position. The cart can move according to the imposed set-point. Different changes have been considered for the set-point. The first one is performed at $t = 35$ s in order to reach $x_{ref} = 0.2$ m. The second set-point change occurs at $t = 70$ s to attain $x_{ref} = 0.2$ m. Figures 19 and 20 show the results obtained respectively with MOIF and MOPIF controllers for a set-point tracking. We note that after the swing up of the pendulum, the IP-C system is successfully stabilized and tracks perfectly the imposed trajectory.

A comparative analysis involving MOIF and MOPIF controllers, along with FOC from a previous study, is conducted. Performance metrics, including overshoots (M_p), settling times (t_r), cart tracking position errors $e(x)$, and the mean value of the control signal U_m, are summarized in Table 3. The MOPIF

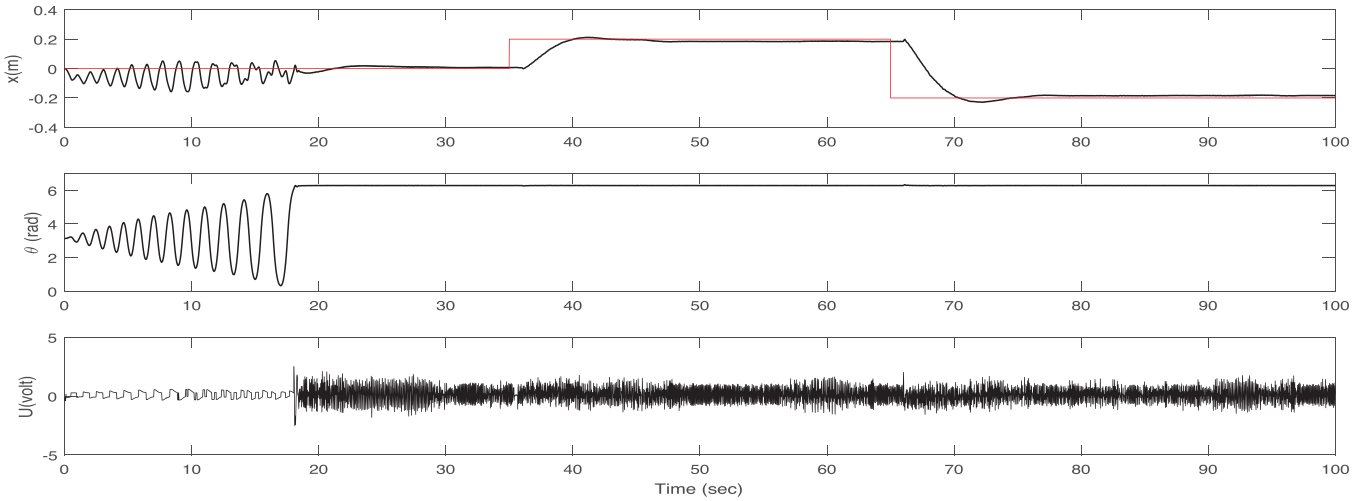

FIGURE 19 Evolution of the position (X),the angle (θ) and the control signal (U_{m}) in the case of MOIF controller.

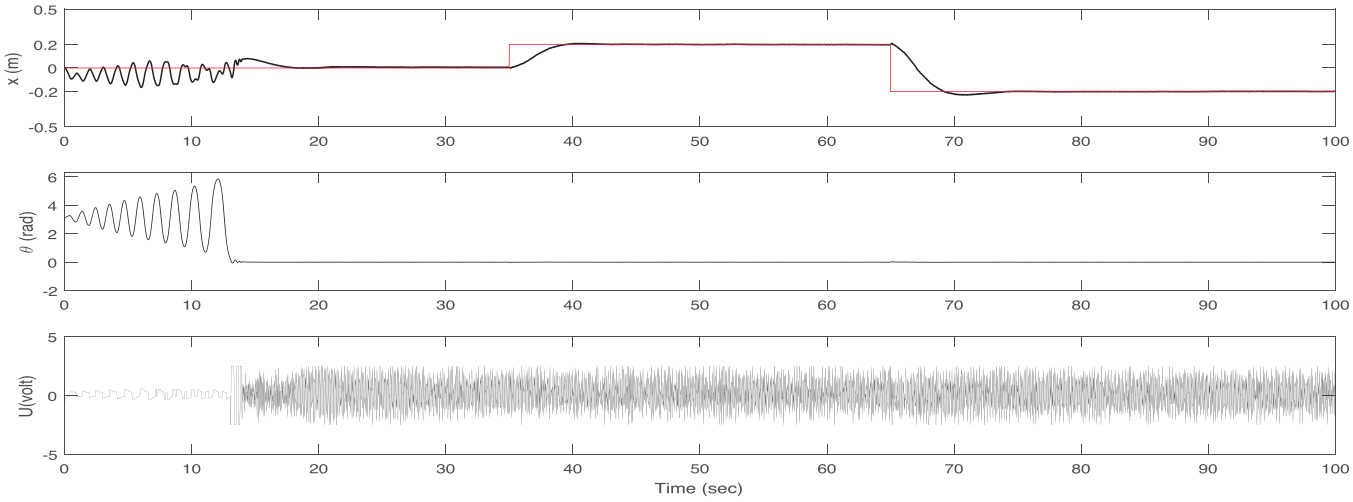

FIGURE 20 Evolution of the position (X), the angle (θ) and the control signal (U_{m}) in the case of MOPIF controller.

controller emerges as the optimal choice, showcasing superior performance metrics across the board. With the lowest overshoot (4%), shortest rise time (4.15 s), and minimal position error (10^{-4}), MOPIF demonstrates enhanced stability, faster response, and greater precision in comparison to the MOIF controller with higher overshoot (14), longer rise time (9 s), and larger position error (3.10^{-4}). The FOC shares a similar control effort with MOIF (0.1 V)but exhibits higher overshoot (28.8%) and longer rise time (7 s), indicating a less favourable transient response. Overall, MOPIF emerges as the preferable choice, offering an optimal balance of dynamic response, accuracy, and stability for the control of the IP-C system.

6 | CONCLUSION

This paper introduces an innovative approach to optimize the parameters of MOIF and MOPIF controllers using a multi-objective PSO algorithm. The primary objective of the optimization process is to minimize three critical performance metrics: integral time absolute error, overshoot, and the Buslowicz stability criterion. This optimization addresses the unique challenges associated with asymptotic stability in non-commensurate order systems.

The proposed controllers have been applied to stabilize an inverted pendulum-cart system and for set-point tracking. A comparative simulation was conducted, involving PID and FOPID controllers, providing valuable insights into the superior performance of the proposed MOIF and MOPIF controllers. The results demonstrated distinct advantages in terms of stability and tracking precision. Numerical evaluations underscored notable progress, indicating a significant decrease in both overshoot and settling time. Notably, the MOPIF controller stood out with an impressive 27% reduction in overshoot and a 4% improvement in settling time compared to the FOPID controller.

To further evaluate the controllers' robustness, additional simulations were carried out. These simulations specifically examined the performance of the controllers in rejecting impulse and step disturbances, as well as their response to variations in the cart mass. The robustness analysis sheds light on the controllers' ability to maintain stability and effective control under challenging conditions.

Experimental implementation on an inverted pendulum-cart system showcased substantial improvements in both stability and reference tracking compared to traditional Fractional-Order Control (FOC). Numerical assessments underscored these advancements, revealing a significant reduction in integral time absolute error and overshoot. Notably, the MOPIF controller exhibited a remarkable 35% decrease in overshoot, contributing to an enhanced dynamic response.

The numerical results not only validate the effectiveness of the proposed optimization method but also highlight tangible benefits in terms of performance and robustness enhancement for fractional-order controllers in dynamic systems, such as the inverted pendulum-cart.

AUTHOR CONTRIBUTIONS

Fatima Cheballah: Conceptualization; formal analysis; investigation; methodology; validation; writing—original draft. **Rabah Mellah**: Conceptualization; methodology; supervision; writing—review and editing. **Abdelhakim Saim**: Methodology; visualization; writing—review and editing.

CONFLICT OF INTEREST STATEMENT

The authors declare no conflict of interest.

DATA AVAILABILITY STATEMENT

Data available on request from the authors.

ORCID

Fatima Cheballah https://orcid.org/0009-0008-7346-4574

REFERENCES

1. Prasad, L.B., Tyagi, B., Gupta, H.O.: Modelling and simulation for optimal control of nonlinear inverted pendulum dynamical system using pid controller and LQR. In: 2012 Sixth Asia Modelling Symposium, pp. 138–143. IEEE, Piscataway, NJ (2012)
2. Prasad, L.B., Tyagi, B., Gupta, H.O.: Optimal control of nonlinear inverted pendulum system using PID controller and LQR: performance analysis without and with disturbance input. Int. J. Automat. Comput. 11, 661–670 (2014)
3. Hazem, Z.B., Bingül, Z.: Comprehensive review of different pendulum structures in engineering applications. IEEE Access 11, 42862–42880 (2023)
4. Bettayeb, M., Boussalem, C., Mansouri, R., Al Saggaf, U.: Stabilization of an inverted pendulum-cart system by fractional pi-state feedback. ISA Trans. 53(2), 508–516 (2014)
5. Mansouri, R., Bettayeb, M., Boussalem, C., Alsaggaf, U.: Linear integer order system control by fractional PI-state feedback. In: Fractional calculus: Applications, pp. 65–91. Nova Science Publishers, Hauppauge, NY (2015)
6. Al-Saggaf, U.M., Mehedi, I.M., Mansouri, R., Bettayeb, M.: State feedback with fractional integral control design based on the Bode's ideal transfer function. Int. J. Syst. Sci. 47(1), 149–161 (2016)
7. Hammouche, S., Mansouri, R., Maidi, A., Bettayeb, M.: New fractional-order LADRC scheme based on a novel filtered-Bode's ideal transfer function for integer-order systems. Mechatronics 93, 103004 (2023)
8. Matignon, D.: Stability results for fractional differential equations with applications to control processing. In: Computational Engineering in Systems Applications. vol. 2, pp. 963–968. ScienceOpen, Lexington, MA (1996)
9. Sabatier, J., Moze, M., Farges, C.: On stability of fractional order systems. Paper presented at the third IFAC workshop on fractional differentiation and its applications, Ankara, 5–7 Nov 2008
10. Casagrande, D., Krajewski, W., Viaro, U.: On the robust stability of commensurate fractional-order systems. J. Franklin Inst. 359(11), 5559–5574 (2022)
11. Busłowicz, M.: Stability analysis of continuous-time linear systems consisting of n subsystems with different fractional orders. Bull. Polish Acad. Sci. Tech. Sci. 60(2), 279–284 (2012)
12. Buslowicz, M.: Stability analysis of linear continuous-time fractional systems of comensurate order. J. Automat. Mob. Robot. Intell. Syst. 12–17 (2013)
13. Stanisławski, R., Latawiec, K.: A modified Mikhailov stability criterion for a class of discrete-time noncommensurate fractional-order systems. Commun. Nonlin. Sci. Numer. Simul. 96, 105697 (2021)
14. Zhong, Y., Gao, J., Zhang, L.: Fractional-order feedforward control method for permanent magnet linear synchronous motor based on frequency-domain adjustment theory. Mech. Syst. Signal Process. 190, 110115 (2023)
15. Kalogirou, S.A.: Artificial intelligence for the modeling and control of combustion processes: a review. Prog. Energy Combust. Sci. 29(6), 515–566 (2003)
16. Liu, X., Jiang, D., Tao, B., Jiang, G., Sun, Y., Kong, J., et al.: Genetic algorithm-based trajectory optimization for digital twin robots. Front. Bioeng. Biotechnol. 9, 1433 (2022)
17. Gandomi, A.H., Yang, X.S., Alavi, A.H.: Cuckoo search algorithm: a metaheuristic approach to solve structural optimization problems. Eng. Comput. 29(1), 17–35 (2013)
18. Roni, M.H.K., Rana, M., Pota, H., Hasan, M.M., Hussain, M.S.: Recent trends in bio-inspired meta-heuristic optimization techniques in control applications for electrical systems: a review. Int. J. Dyn. Cont. 10, 999–1011 (2022)
19. Gad, A.G.: Particle swarm optimization algorithm and its applications: a systematic review. Arch. Comput. Methods. Eng. 29(5), 2531–2561 (2022)
20. Shami, T.M., El Saleh, A.A., Alswaitti, M., Al Tashi, Q., Summakieh, M.A., Mirjalili, S.: Particle swarm optimization: a comprehensive survey. IEEE Access 10, 10031–10061 (2022)
21. Wang, D., Tan, D., Liu, L.: Particle swarm optimization algorithm: an overview. Soft Comput. 22(2), 387–408 (2018)
22. Aboud, A., Rokbani, N., Fdhila, R., Qahtani, A.M., Almutiry, O., Dhahri, H., et al.: DPb-MOPSO: a dynamic pareto bi-level multi-objective particle swarm optimization algorithm. Appl. Soft Comput. 129, 109622 (2022)
23. Goud, H., Sharma, P., Nisar, K., Ibrahim, A., Haque, M., Yadav, N., et al.: PSO based multi-objective approach for controlling PID controller. Comput. Mater. Contin. 71(3), 4409–4423 (2022)
24. Ngatchou, P., Zarei, A., El Sharkawi, A.: Pareto multi objective optimization. In: Proceedings of the 13th International Conference on, Intelligent Systems Application to Power Systems, pp. 84–91. IEEE, Piscataway, NJ (2005)
25. Wang, H., Liang, M., Sun, C., Zhang, G., Xie, L.: Multiple-strategy learning particle swarm optimization for large-scale optimization problems. Complex Intell. Syst. 7, 1–16 (2021)
26. Reynoso Meza, G., Blasco, X., Sanchis, J., Martinez, M.: Controller tuning using evolutionary multi-objective optimisation: current trends and applications. Cont. Eng. Pract. 28, 58–73 (2014)
27. Daou, R.A.Z., Moreau, X.: A comparison between integer order and fractional order controllers applied to a hydro-electromechanical system. Trans. Cont. Mech. Syst. 2(3), 131–143 (2013)
28. Betala, R., Nangrani, S.: Comparison of performance of fractional order PID controller with conventional controller for industrial applications. In: 2023 IEEE International Conference on Integrated Circuits and

Communication Systems (ICICACS), pp. 1–6. IEEE, Piscataway, NJ (2023)
29. Lloyds Raja, G., Ali, A.: New PI–PD controller design strategy for industrial unstable and integrating processes with dead time and inverse response. J. Cont. Autom. Elect. Syst. 32, 266–280 (2021)
30. Busłowicz, M., Kaczorek, T.: Simple conditions for practical stability of positive fractional discrete-time linear systems. Int. J. Appl. Math. Comput. Sci. 19(2), 263–269 (2009)
31. Almeida, R., Tavares, D., Torres, F.: The Variable-Order Fractional Calculus of Variations. Springer, Cham (2019)
32. Podlubny, I.: Fractional-order systems and $PI^{\lambda}D^{\mu}$-controllers. IEEE Trans. Autom. Cont. 44(1), 208–214 (1999)
33. Matignon, D.: Stability properties for generalized fractional differential systems. In: ESAIM: Proceedings, vol. 5, 145–158. EDP Sciences, Les Ulis (1998)
34. Mishra, S.K., Chandra, D., et al.: Stabilization and tracking control of inverted pendulum using fractional order PID controllers. J. Eng. 2014, 752918 (2014)

How to cite this article: Cheballah, F., Mellah, R., Saim, A.: Design of fractional MOIF and MOPIF controller using PSO algorithm for the stabilization of an inverted pendulum-cart system. IET Control Theory Appl. 1–16 (2024). https://doi.org/10.1049/cth2.12648